Range-Extended GPS Kinematic Positioning Using Numerical Weather Prediction Model

Felipe Nievinski[1]
Karen Cove[1]
Marcelo Santos[1]
Dave Wells[1, 2]
Robert Kingdon[1]

[1] *Department of Geodesy and Geomatics Engineering, University of New Brunswick, Canada*
[2] *Department of Marine Science, University of Southern Mississippi, USA*

BIOGRAPHY

Felipe Nievinski is a M. Sc. E. student and research assistant at the Dept. of Geodesy and Geomatics Engineering, University of New Brunswick. His supervisor is Dr. Marcelo Santos. At the end of 2004 he received his Geomatics Engineering degree from the Federal University of Rio Grande do Sul, Brazil. He is mainly interested in computational problems in geodesy.

Karen Cove received her B. Sc. in Geomatics Engineering in 2002 and her M. Sc. E. in 2005 from the Dept. of Geodesy and Geomatics Engineering at the University of New Brunswick, Canada. Her research interests include GPS positioning and marine boundaries.

Marcelo Santos is Associate Professor at the Dept. of Geodesy and Geomatics Engineering at UNB. He holds a M. Sc. in Geophysics from the National Observatory, in Rio de Janeiro, and a Ph.D. in Geodesy from UNB. He has been involved in research in the fields of space and physical geodesy, GNSS and navigation.

Dave Wells is Professor Emeritus in the Dept. of Geodesy and Geomatics Engineering at UNB, as well as Professor in the Dept. of Marine Science at the University of Southern Mississippi (USM), and Adjunct Professor in the Center for Coastal and Ocean Mapping at the University of New Hampshire. Dave's academic interests include geodesy, applied bathymetry, kinematic positioning, water levels and tides, and hydrographic data management.

Robert Kingdon is a research assistant at the Department of Geodesy and Geomatics Engineering, University of New Brunswick. He completed his undergraduate degree with the Department in May, 2005; and, pending funding, will begin a Master's degree in the same discipline, in September. As a research assistant, he assists with GPS processing; although his primary interest is with physical geodesy. He is working under Dr. Marcelo Santos.

ABSTRACT

We have continued in our effort to investigate the use of Numerical Weather Prediction (NWP) models in GPS positioning, in an attempt to obtain better prediction of tropospheric delay. We have expanded our previous work on deriving zenith path delays from the Canadian GEM NWP model to obtain slant path delays, via ray-tracing in the three-dimensional NWP grids. We have developed an algorithm for this purpose. We have tested our approach in the ranging domain, comparing it to slant delays given by the UNB3 model and to zenith hydrostatic delays given by the Saastamoinen model with surface pressure measurements. We have also tested it in the position domain, using real GPS data from the Princess of Acadia Project, in a combination of short- and long-baseline solutions. Even though preliminary, our results indicate that (i) there is no advantage in ray-tracing for elevation angles greater than 30º, and (ii) NWP is equivalent to UNB3 for decimetre-level positioning. Further comparisons are needed to assess the performance of the GEM NWP model at higher precision levels.

INTRODUCTION

GPS radio signals are refracted when they propagate through the Earth's neutral atmosphere. Timings (rangings) of GPS signals are delayed (increased) compared to what would be measured if the signals were propagating in a vacuum. In other words, the distance measured with GPS signals propagating through the neutral atmosphere (the bulk of which is the troposphere but also includes the stratosphere) is always greater than the geometrical distance between satellite's and receiver's antennas.

Those delays range from 2.3 m at zenith to approximately 26 m at 5º-elevation angle (Seeber, 2003). They introduce non-negligible errors in the estimates derived from GPS observations and must be taken into account in precise applications.

The neutral atmosphere propagation delays are better analyzed separating them in two components, a hydrostatic one (also called dry) τ_h and a non-hydrostatic one (also called wet) τ_{nh} (Langley, 1996):

$$\tau = \tau_h + \tau_{nh}.$$

The hydrostatic delay accounts for approximately 90% of the total delay and is fortunately highly predictable from surface pressure measurements. The non-hydrostatic component is function of humidity, hence highly variable and harder to predict.

Most of currently used prediction models are a compound model, made of (i) a zenith delay prediction model and (ii) a mapping function. (i) is usually based on limited lookup tables to get the weather parameters at a given position. (ii) maps the delay at zenith to lower elevation angles. To name but a few, we cite (i) Saastamoinen (as given by Davis et al., 1985), (ii) Niell's mapping function (Niell, 1996), and UNB3 (Collins and Langley, 1999) as a compound model.

Due to the prediction capability of current models, it has been recommended that, for precision applications, only the hydrostatic component be predicted and that the non-hydrostatic component (actually its mapping to zenith) be estimated as an unknown parameter in the adjustment of GPS observations (McCarthy and Petit, 2004).

One possibly better model for humidity and hence non-hydrostatic delay is that of Numerical Weather Prediction (NWP) models (Pany et al., 2001; Jensen, 2002). Global and regional NWP models are produced daily by many meteorological agencies throughout the world, mainly for weather forecasting purposes. That possibility is based on the fact that NWP models, especially the regional ones, have a much higher resolution than the lookup tables on which the current prediction models are based.

As part of an ongoing investigation to integrate NWP models in GPS processing at UNB (Cove et al., 2004; Cove, 2005), we calculated slant-path delays from a NWP model and started to test them both in the range domain and in the position domain.

The testing in the position domain was done as part of the Princess of Acadia project, which we describe in the next section. In the following section we summarize how we calculated slant-path delays from a NWP model, and in the two remaining sections we describe the test and comparisons done and analyze the results. We close this paper with conclusions and an indication of current and future goals in this investigation.

PRINCESS OF ACADIA PROJECT

The Princess of Acadia Project consists of a range of activities, which started with a data collection campaign around the Bay of Fundy, located between the Canadian Provinces of New Brunswick and Nova Scotia, in Eastern Canada. Data from a network of GPS receivers, meteorological stations and tide gauges were collected for a period of over one year (from November 2004 to December 2004). The long-term data collection allows the data to cover different seasons and distinct passing of weather fronts.

A receiver was also set up on board the ferry Princess of Acadia, which connects the cities of St. John, New Brunswick, and Digby, Nova Scotia, as many as 3 times a day. The Bay of Fundy was a very convenient choice due to its proximity to UNB but most importantly due to the fact that it possesses tides of high amplitude, providing an additional vertical dynamics to the project.

Figure 1 shows the geographic location of the project, with indication of the stations used and their respective distances. The ferry travels the 74 km line between Digby (DRHS) and Saint John (CGSJ). These stations were implemented solely to serve the project. Other stations shown are Fredericton (FDRN) and Halifax (HLFX). The latter stations belong to the Canadian Active Control System, maintained by NRCan.

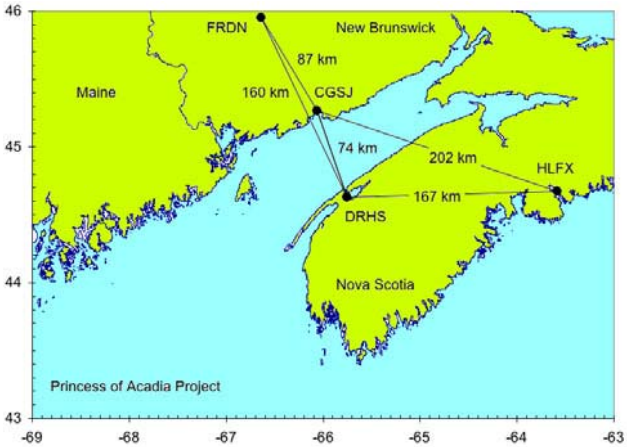

Fig. 1: The Princess of Acadia Project location.

A number of issues have been dealt with in this project, dealing with variability in positioning due to area coverage and due to weather fronts, issues related to seamless vertical datum and site dependent effects (Santos et al, 2004).

The objectives of the Princess of Acadia Project, as proposed by Santos and Cove (2002), are to investigate:

- Extension in long-range high-accuracy relative kinematic positioning.

- Effect of variability in weather conditions, especially for long baselines, in a marine environment.
- Inter-connections among vertical reference systems, having the ferry as a "moving tide gauge".
- Local effects, such as multipath effect on base stations and on the rover receiver, and tidal effects such as body tides and ocean tidal loading, and how they impact relative kinematic positioning.

As data collection is over we are moving ahead with analysis of the data in the light of the project objectives. The investigation on the use of Numerical Weather Prediction (NWP) model data is an attempt to obtain a better representation of the neutral atmosphere, to satisfy two of our project objectives: extend the range in high-accuracy kinematic positioning with a more realistic representation of weather conditions affecting the observations.

CALCULATION OF SLANT-PATH DELAYS FROM NWP MODELS

We used the regional high-resolution version of the Global Environmental Multiscale NWP model, developed by the Meteorological Research Branch in partnership with the Canadian Meteorological Centre of Environment Canada (Côté et al, 1998). That model describes each weather parameter (e.g., temperature, humidity) as a three-dimensional gridded field. Those fields are made of 28 isobaric levels at standard pressure values, and some fields have an additional ground surface level. Even though the regional model is run on a variable-step grid with a 15 km central core resolution, the fields are made available on a polar-stereographic horizontal grid with a 15 km resolution at 60°N. All fields are available at 3-hourly intervals.

The delay τ is given by the line integral of refractivity N along the curved ray path, from the satellite to the receiver:

$$\tau = 10^{-6} \int_C N(\ell) d\ell,$$

where τ is in metres. We approximated the curved ray path by a straight-line path, namely the direction between satellite and receiver, and evaluated that integral numerically. N is sampled at as many points as needed to fulfill the tolerance specified (e.g., 1 mm). A typical curve of refractivity versus distance from the receiver towards the satellite (with 0.1 mm tolerance) is shown in fig. 2.

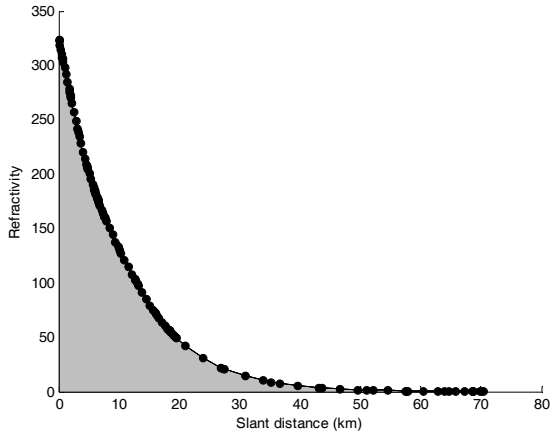

Fig. 2: Typical curve of refractivity versus slant distance, from receiver towards satellite. Elevation angle is 45º. Black dots represent points at which refractivity was sampled.

The refractivity N at a given distance ℓ along the path is obtained interpolating the weather parameters at the corresponding three-dimensional position in the NWP gridded fields. As the GEM NWP models goes up to approximately 20 km in the vertical direction, we supplemented it with the COSPAR International Reference Atmosphere (CIRA-86) model, described in Fleming et al. (1988). We used it for heights above the NWP model and up to 50 km, over which we should not expect delay due to the neutral atmosphere (Langley, 2005).

The interpolated values for temperature T, pressure P, and specific humidity s are applied, after proper conversion, in the following formula (Langley, 1996):

$$N = K_1\left(\frac{P_d}{T}\right)Z_d^{-1} + \left[K_2\left(\frac{e}{T}\right) + K_3\left(\frac{e}{T^2}\right)\right]Z_w^{-1},$$

where $P_d = P - e$ is the partial pressure for dry gases (Seeber, 2003) and $e = sp/(0.622 + 0.378s)$ is the water vapor pressure (Rocken et al., 2001). The compressibility factors Z_d^{-1} and Z_w^{-1} were both set to one because "for typical conditions in the earth's atmosphere, [they] depart from unity by less than 1 part in 10^3" (Langley, 1996). The terms K_1, K_2, and K_3 are empirically determined coefficients, whose values used in this paper are 76.6, 64.8, and 3.776×10^5 respectively.

A key step in the computation of the slant path delays is the transformation of coordinates from the integration space (ℓ) to the interpolation space (x, y, H^G), where x, y represent horizontal coordinates in the polar-stereographic projection and H^G is geopotential height. The transformation to the horizontal components (x, y) is

made of only well-known transformations (namely, cartesian geocentric to geodetic curvilinear to projected coordinates). The transformation to the vertical component $\left(H^G\right)$ is described in the Appendix A.

TESTING IN THE RANGE DOMAIN

NWP compared to UNB3 as function of elevation angle

We compared slant delays given by the NWP to slant delays given by the UNB3 prediction model. Figures 3a, 3b, 3c show, respectively, the total, hydrostatic, and non-hydrostatic NWP delay and their corresponding discrepancies w.r.t. UNB3. All values are for the IGS station UNB1, on May 20, 2005, 0h UTC, North azimuth. In that particular case, NWP slant delays were always smaller than UNB3 slant delays. We analyzed only elevation angles higher than 10º. The discrepancies at zenith in total, hydrostatic, and non-hydrostatic delay were -0.047 m, -0.013 m, -0.033 m, respectively. As expected, the discrepancies for the hydrostatic component were smaller than the discrepancies for the non-hydrostatic component.

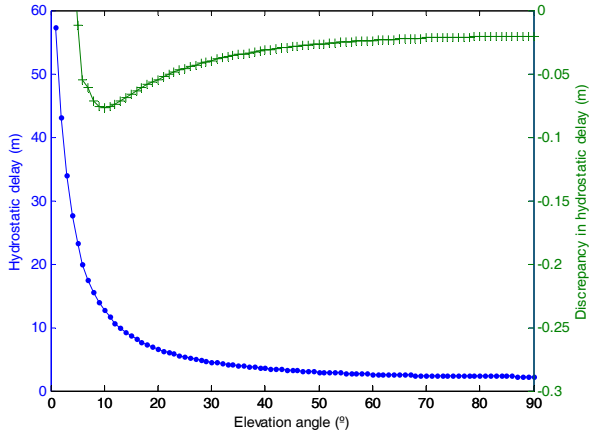

Fig. 3a: Hydrostatic delay.

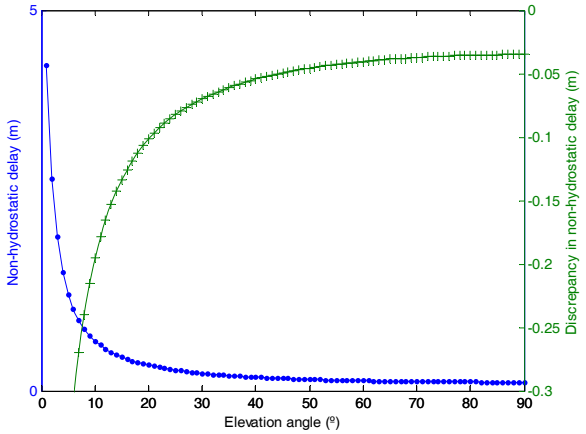

Fig. 3b: Non-hydrostatic delay.

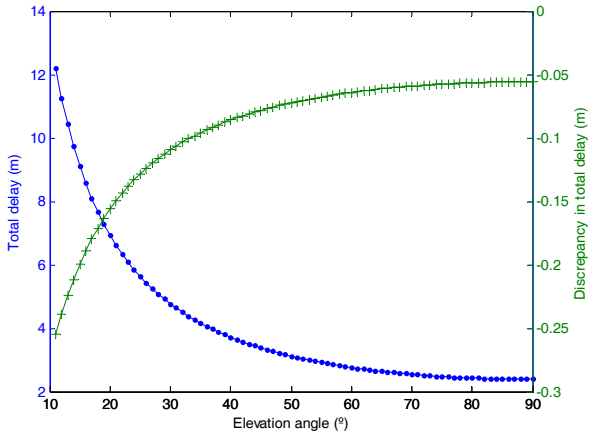

Fig. 3c: Total delay.

Fig. 3: NWP predictions (dots) and respective discrepancies (crosses) w.r.t. UNB3 predictions. At station UNB1, on May 20, 2005.

NWP compared to UNB3 and Saastamoinen at IGS stations – zenith hydrostatic delays

A second comparison was performed with respect to zenith hydrostatic delays (ZHD). The justification for comparing ZHD is that they are highly predictable from surface pressure measurements.

We used all IGS stations inside the GEM NWP extents, with meteorological data (RINEX MET files) on May 20, 2005, 0h UTC, and with known values for their height above the ground (that information is required in our calculation of delays). The IGS codes of those stations are listed in table 1.

Tab. 1: code of IGS stations used in the second comparison.

1	ALGO	6	REYK
2	CHUR	7	SCH2
3	KUUJ	8	STJO
4	PRDS	9	WHIT
5	QAQ1	10	YELL

We considered the values calculated with Saastamoinen model using the meteorological files (denoted Saas MET) as benchmark values. We compared also UNB3 and Saastamoinen using pressure taken from the NWP at the receiver (denoted Saas NWP).

The result of this comparison is shown in figures 4a and 4b. Figure 4a shows the actual values given by each one of the models. Figure 4b shows their differences with respect to Saas MET. These figures indicate that, even though there is a good overall agreement among the

predictions, there are significant discrepancies (up to 6 cm at station # 9).

It is interesting to note that the curves for NWP and Saas NWP are always close together. That indicates that our approach for calculating delays closely approximates the Saastamoinen model for the hydrostatic delay.

It is interesting to note also that the only difference between Saas MET and Saas NWP is the value used for pressure at the receiver. The fact that those two curves are not close together indicates that we are not getting the correct value for pressure at the receiver. In future works we will investigate if that is due to a faulty transformation to vertical coordinates or due to mismodeling of the pressure field by the NWP model.

A consequence of the two facts above is that once the separation between Saas NWP and Saas MET is corrected, the separation between NWP and Saas MET (benchmark) will be corrected too.

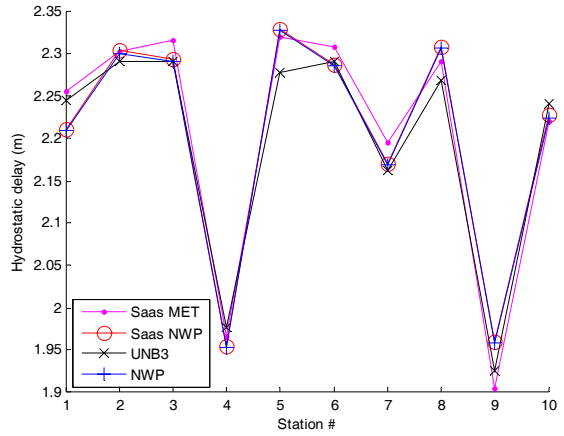

Fig.4a: Hydrostatic delay as predicted by a number of models, at IGS stations, on May 20, 2005.

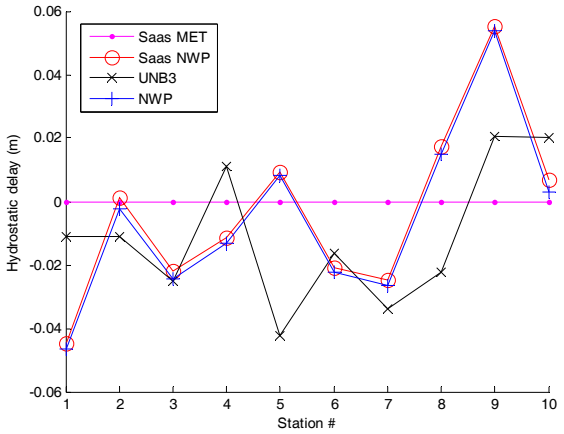

Fig.4b: Discrepancy in hydrostatic delay with respect to Saas MET, at IGS stations, on May 20, 2005.

NWP slant delays compared to NWP zenith delays + Niell's mapping function

A third comparison was made, between NWP slant total delays and NWP zenith total delay mapped to lower elevation angles using Niell's mapping function (Niell, 1996).

Even though each result is computed in a completely different manner, the discrepancy between the two is smaller than 1mm for elevations between 90º and 30º and smaller than 1 cm between 30º and 20º. Below 10º the discrepancy grows fast, reaching 2m at 1º and a singularity at 0º (not shown in the figure).

The main practical conclusion of this result is that, for that particular occasion and considering a precision of 1 mm, there is no advantage in calculating slant delays directly – calculating a single zenith delay and using it with a mapping function gives equivalent results and it is a lot faster to process.

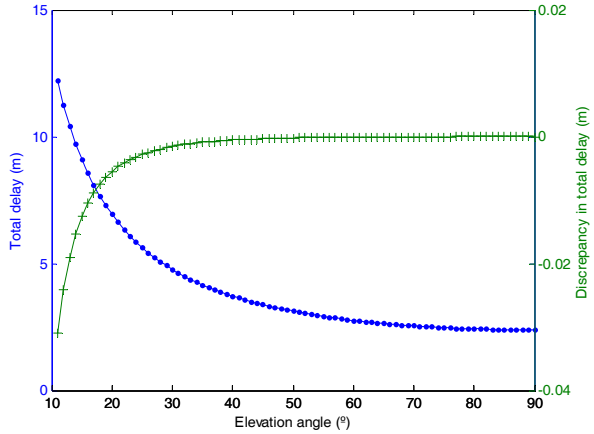

Fig. 5: Total delay (dots) and discrepancy in total delay (crosses), NWP vs. NWP+NMF.

TESTING IN THE POSITION DOMAIN

The tests done in the position domain used data from the Princess of Acadia Project. We formed two baselines to the same rover receiver (installed on the ferry), one short (~4km) and one long (~74 km). In both baselines we constrained the static station and estimated the coordinates of the rover for each epoch. The short-baseline solution was used as the reference solution, and the different long-baseline solutions were compared to it.

The data sets were processed fixing ambiguities for the short-baseline and using the iono-free linear combination for the long-baseline. We used the software tool GrafNav, of WayPoint Consulting, version 7.6.

We had three long-baseline solutions, which differed by the way we dealt with the troposphere: (i) uncorrected

(using no prediction model), (ii) corrected using NWP, and (iii) corrected using UNB3. In the latter two cases we subtracted the predicted delays from the raw GPS observations and generated a "corrected" observation file. We processed only a short session, 1 hour long, at 10s sampling rate (not making use of the 1 Hz sampling rate data available). During this period the ferry was docked in the Digby ferry terminal, but it was still subject to small movements, such as tides.

Satellite residuals

First we looked at the double-difference carrier-phase residuals. They were significantly reduced, as can be seen in figures 6a, 6b, and 6c and also by the RMS values shown in table 2. The difference between NWP and UNB3 solutions is not significant, though.

Tab. 2: RMS values of long-baseline solutions.

Uncorrected	2.06 cm
NWP	1.27 cm
UNB3	1.28 cm

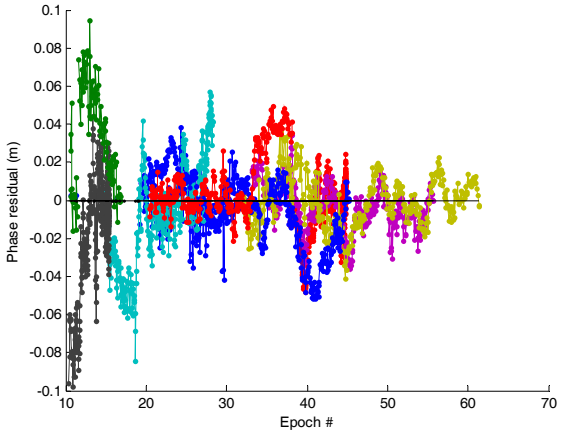

Fig.6a: Uncorrected observations

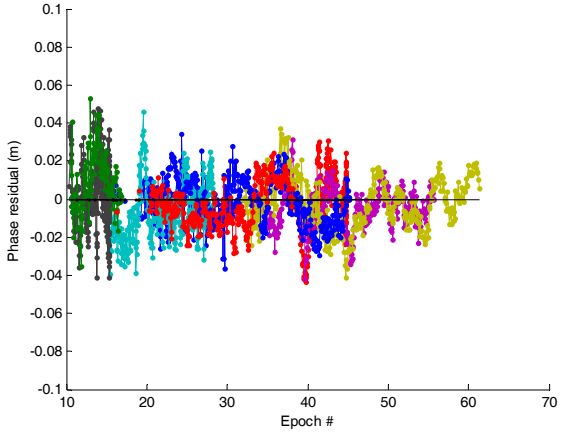

Fig.6b: NWP-corrected observations.

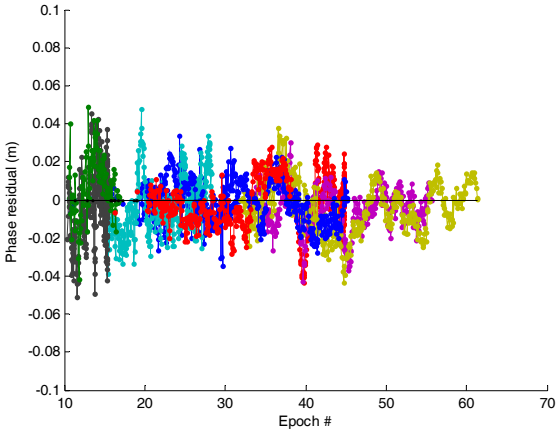

Fig.6c: UNB3-corrected observations.

Fig. 6: Phase residuals versus elevation angle (the residuals for each individual satellite are shown in a different color).

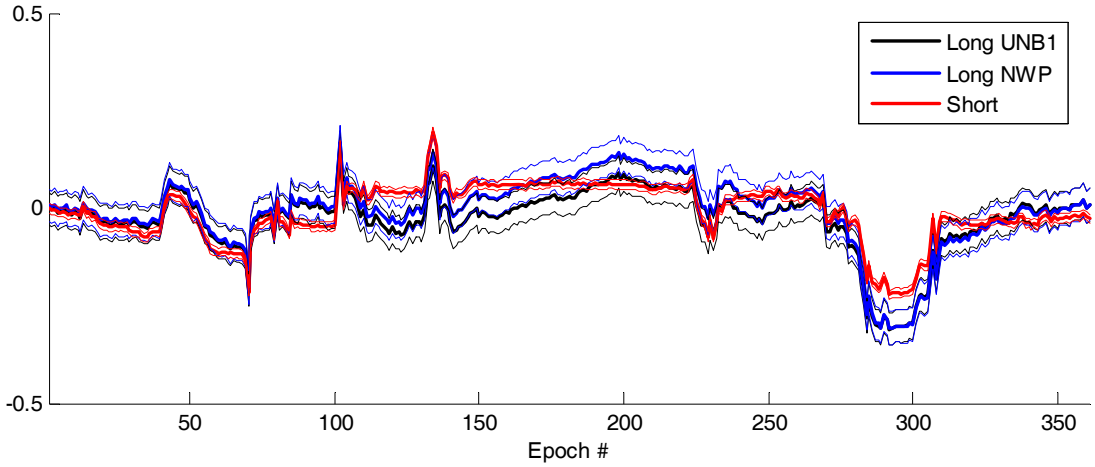

Fig. 7a: Latitude

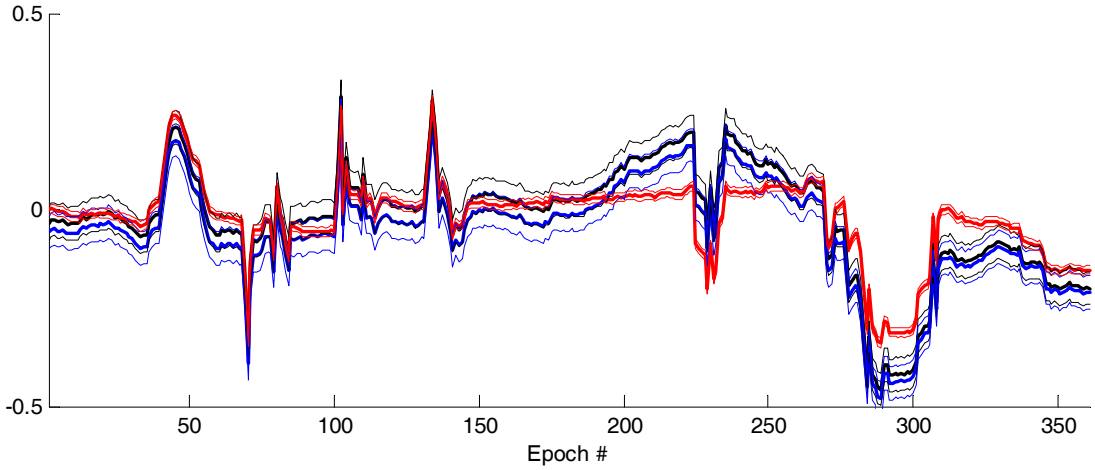

Fig. 7b: Longitude.

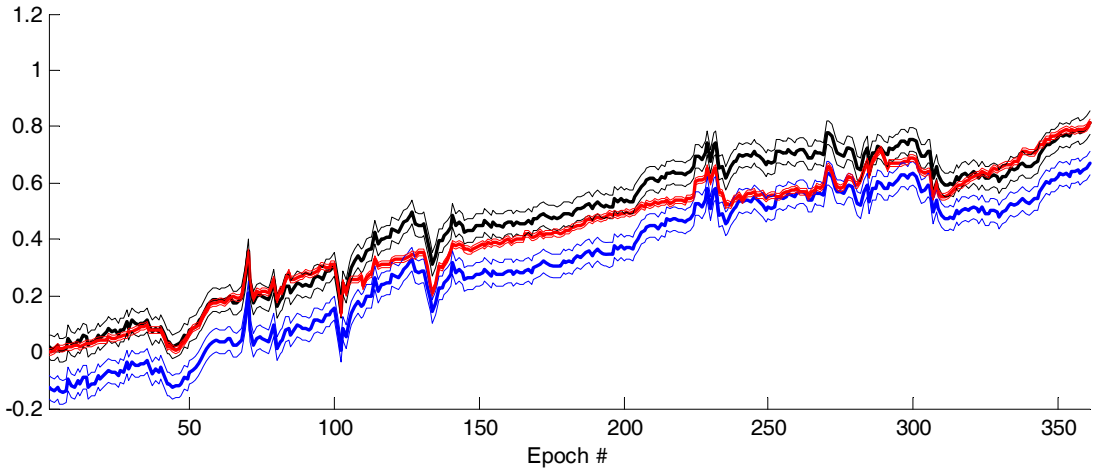

Fig. 7c: Height.

Fig. 7: Rover solutions (bold lines) and 1-sigma curves (thin lines) for short-baseline solution (solid line), NWP long-baseline (dashed line), and UNB3 long-baseline solution (dotted line).

Position time-series

Figures 7a, 7b, and 7c show time-series of the short-baseline solution (named "Short") and of the different long-baseline solutions (named "Long UNB3" and "Long NWP"). Clearly, the UNB3 and NWP solutions for horizontal components (latitude and longitude) overlap significantly at 1-sigma. The long-baseline solutions for the vertical component are better separated, but the reference solution (short-baseline) wanders between the two.

Position statistics

The statistic we are focused on is the bias. Table 3 shows, on one hand, a smaller horizontal bias for the NWP solution (0.7 cm) than that of the UNB3 solution (1.9 cm); on the other hand, the bias for the NWP vertical solution (-10.0 cm) is greater than that of the UNB3 solution (5.0 cm). Yet, when we analyze those statistics in shed of their standard deviations (obtained by formal propagation of the standard deviation for each solution), we realize that their difference is not statistically significant (at 1-sigma in the horizontal and at 1.5-sigma in the vertical component).

Tab. 3: Statistics for the discrepancy of the three long-baseline solutions with respect to the short-baseline, solution for position of rover receiver.

	RMS (cm)		Bias (cm)		Correlation
	Horiz	Vert	Vert	Horiz	Vert
Uncorrected	10.7	-9.8	-9.8 +/- 6.2	7.6 +/-3.6	0.861
NWP	4.5	-10.0	-10.0 +/-6.8	0.7 +/-3.5	0.983
UNB3	4.9	5.0	5.0 +/-6.8	1.9 +/-4.5	0.977

There is no result in the position domain that allows us to discriminate between NWP and UNB3 solutions and point out which prediction model is better, for decimetre-level applications such as this. Since there is a high computational cost associated with the calculation of slant path delays from NWP models, the UNB3 prediction model might be preferred for decimeter-level applications.

CONCLUSIONS AND FUTURE WORK

We have computed slant path delays from the GEM Numerical Weather Prediction model. We have tested those delays in the ranging domain, comparing them to UNB3 and Saastamoinen prediction models. We have also tested them in the position domain processing real GPS data.

The results shown in this paper are our first ones related to slant delays and portray a work in progress. Even though preliminarily, our main conclusions are that (i) there is no advantage in ray-tracing for elevation angles greater than 30º, and (ii) NWP is equivalent to UNB3 for decimetre-level positioning.

Further comparisons are needed to assess the performance of the NWP model at higher precision levels. As future work, we will (i) further investigate the transformation to geopotential heights, because it may be introducing biases at the centimetre level; (ii) process static baselines, which would provide precision enough to allow us to discriminate between NWP and UNB3 solutions; (iii) insert the delays in the adjustment or filter level, with proper constraints, instead of modifying the raw observations; and (iv) extend the NWP predictions to elevation angles below 10º.

ACKNOWLEDGMENTS

The first author acknowledges financial support from the Canadian International Development Agency (CIDA). He also acknowledges the Institute of Navigation for providing a travel grant to attend the ION Annual Meeting.

The data collection within the Princess of Acadia Project was possible due to funds from the Office of Naval Research, through the University of Southern Mississippi, and from the National Science and Engineering Research Council of Canada (NSERC), through the Discovery Grant of the third author of this paper.

Thanks to the Canadian Meteorological Centre for granting us access to its GEM NWP high-resolution model.

APPENDIX A – Transformation to geopotential heights

The geopotential height H^G at a point *P,* as used in the NWP model, is obtained evaluating the following equation (Vedel, 2000):

$$H^G = H_S^G - \frac{1}{g_0}\int_{\ln p_s}^{\ln p'} RT\, d\ln p$$

where H_S^G is the geopotential height on the ground surface, p' and p_S are respectively pressure at the point *P* and on the ground, *R* is the gas constant, *T* is temperature, and "$g_0 = 9.80665\ \mathrm{m/s^2}$ is a value decided upon the WMO [World Meteorological Organization] and used by all meteorological offices" (Vedel, 2000, p. 3). That integral is evaluated along the vertical direction, from the ground up to the point *P*. The second term has a negative sign in front of it because pressure decreases upwards, while

height increases. The NWP model gives H^G only at its gridded nodes.

To obtain H^G at any other point P at any distance ℓ from the receiver, ideally we should evaluate that same equation. The problem is that we do not know the upper limit of that integral, i.e., the pressure p' at the given point P.

Vedel (2000) re-wrote that integral in terms of gravity g, by assuming hydrostatic equilibrium,

$$dp = -\rho g\, dH,$$

and combining it with the equation of state:

$$p = \rho R T,$$

where ρ is density, g is gravity (unsigned), and H is orthometric height. He obtained the following expression:

$$H^G = H_S^G - \frac{1}{g_0}\int_{H_S}^{H'} g(H)\,dH,$$

where H' and H_S are respectively orthometric height at the point P and on the ground surface. He goes on and derives an expression for g and evaluates that integral numerically.

Instead, we re-wrote the expression for H^G again, noting that the integral above is gravity potential W difference; hence:

$$H^G = H_S^G - \frac{1}{g_0}\left[W(H') - W(H_S)\right],$$

or simply:

$$H^G = -\frac{1}{g_0}\left[W - W_0\right],$$

because

$$H_S^G = -\frac{1}{g_0}\left[W(H_S) - W(H=0)\right]$$

where $W(H=0) = W_0 = 62\,636\,856.88\ \mathrm{m}^2/s^2$ is the gravity potential on the geoid. To evaluate W we used the defining constants of the WGS84 ellipsoid model and the EGM96 expansion of the gravitation potential in spherical harmonics (Lemoine et al., 1998).

Finally, we added to H^G a term δH^G to zero a bias between our solution H_S^G and NWP's solution ${}^{NWP}H_S^G$ for H^G on the ground surface:

$$\delta H^G \equiv H_S^G - {}^{NWP}H_S^G,$$

$$H^G = -\frac{1}{g_0}\left[W - W_0\right] - \delta H^G.$$

That term requires us to know the position of the ground surface right under the point P at which we want H^G. We could obtain that using, e.g., a Digital Elevation Model, but for the time being we assume that the bias for any point P equals the bias at the receiver.

REFERENCES

Collins, J. P. and R. B. Langley (1999). Nominal and Extreme Error Performance of the UNB3 Tropospheric Delay Model. Department of Geodesy and Geomatics Engineering Technical Report No. 204, University of New Brunswick, Fredericton, NB. Canada.

Côté, J., S. Gravel, A. Méthot, A. Patoine, M. Roch, A. Staniforth (1998). The Operational CMC–MRB Global Environmental Multiscale (GEM) Model. Part I: Design Considerations and Formulation. *Monthly Weather Review.* Vol. 126, Issue: 6. pp. 1373-1395.

Cove, K., M. C. Santos, D. Wells and S. Bisnath (2004). Improved tropospheric delay estimation for long baseline, carrier phase differential GPS positioning in a coastal environment. *Proceedings of the Institute of Navigation GNSS-2004*, 21-24 September, 2004, Long Beach, CA, USA, pp. 925-932.

Cove, K. (2005). Improvements in GPS tropospheric delay estimation with numerical weather prediction. M.Sc.E. Thesis. Department of Geodesy and Geomatics Engineering, University of New Brunswick, Fredericton, NB, Canada.

Davis, J. L., T.A. Herring, I. I. Shapiro, A.E.E. Rogers, and G. Elgered (1985), "Geodesy by Radio Interferometry: Effects of Atmospheric Modelling Errors on Estimates of Baseline Length," *Radio Science*, 20, No. 6, pp. 1593–1607.

Fleming, E.L., S. Chandra, M.R. Schoeberl and J.J. Barnet, (1988). *Monthly Mean Global Climatology of Temperature, Wind, Geopotential Height and Pressure for 0-120 km*. NASA TM-100697, Goddard Space Flight Center, Greenbelt, Maryland, U.S.A.

Jensen, A.B.O. (2002) Investigations on the use of numerical weather predictions, ray tracing, and tropospheric mapping functions for network RTK. *Proceedings of the Institute of Navigation GPS-2002*, 24-27 September, 2002, Portland, OR, CA, USA, pp. 2324-2333.

Langley, R. (1996). Propagation of the GPS signals. In Kleusberg; Teunissen (Eds.) *GPS for Geodesy* (Lecture Notes in Earth Sciences). Springer. Chap. 3, pp.103-140.

Langley, R. (2005). Personal Communication. Department of Geodesy and Geomatics Engineering Technical Report No. 204, University of New Brunswick, Fredericton, NB. Canada.

Lemoine, F.G., S. C. Kenyon, J. K. Factor, R.G. Trimmer, N. K. Pavlis, D. S. Chinn, C. M. Cox, S. M. Klosko, S. B.

Luthcke, M. H. Torrence, Y. M. Wang, R. G. Williamson, E. C. Pavlis, R. H. Rapp and T. R. Olson. (1998) *The Development of the Joint NASA GSFC and NIMA Geopotential Model EGM96*. NASA Goddard Space Flight Center, Greenbelt, Maryland, 20771 USA. Available at <http://cddis.gsfc.nasa.gov/926/egm96/doc/S11.HTML>.

Pany, T., P. Pesec and G. Stangl (2001). Elimination of tropospheric path delays in GPS observations with the ECMWF numerical weather model, *Physics and Chemistry of the Earth*, Part A: Solid Earth and Geodesy, Vol. 26, Issues 6-8, pp. 487-492.

Santos, M .C. and K. M. Cove (2002). *Carrier phase differential kinematic GPS data analysis*. Final research project report prepared for the University of Southern Mississippi and NAVOCEANO, Fredericton, N. B., June, 60 pp.

Santos, M. C., D. Wells, K. Cove and S. Bisnath (2004). The Princess of Acadia GPS Project: Description and scientific challenges. *Proceedings of the Canadian Hydrographic Conference CHC2004*, 25-27 May, 2004, Ottawa.

Niell, A. E., 1996, "Global Mapping Functions for the Atmosphere Delay of Radio Wavelengths," *J. Geophys. Res.*, 101, pp. 3227–3246.

McCarthy, D.D. Petit, G. (2004) IERS Conventions (2003) (IERS Technical Note # 32). Frankfurt am Main: Verlag des Bundesamts für Kartographie und Geodäsie, 2004. 127 pp., paperback, in print. Available at <http://www.iers.org/iers/publications/tn/tn32/>.

Seeber, G. (2003) *Satellite geodesy*: foundations, methods, and applications. 2nd edition.Walter de Gruyter.

Vedel, H. (2000) *Conversion of WGS84 geometric heights to NWP model HIRLAM geopotential heights*, DMI scientific report 00-04, Danish Meteorological Institute. Available at <http://www.dmi.dk/dmi/sr00-04.pdf>.